RESEARCH ARTICLE

Angiogenic growth factors augment K–Cl cotransporter expression in erythroid cells via hypoxia-inducible factor-1α

Caryn S. Gonsalves,[1,2] Scott Crable,[1] Sharat Chandra,[1] Wei Li,[3] Vijay K. Kalra,[2] and Clinton H. Joiner[1,3]*

The potassium chloride cotransporters (KCC) family of proteins are widely expressed and are involved in the transepithelial movement of potassium and chloride ions and the regulation of cell volume. KCC activity is high in reticulocytes, and contributes to the dehydration of sickle red blood cells. Because plasma levels of both vascular endothelial growth factor (VEGF) and placental growth factor (PlGF) are elevated in sickle cell individuals, and VEGF has been shown to increase KCC expression in other cells, we hypothesized that VEGF and PlGF influence KCC expression in erythroid cells. Both VEGF and PlGF treatment of human erythroid K562 cells increased both mRNA and protein levels of KCC1, KCC3b, and KCC4. VEGF- and PlGF-mediated cellular signaling involved VEGF-R1 and downstream effectors, specifically, PI-3 kinase, p38 MAP kinase, mTOR, NADPH-oxidase, JNK kinase, and HIF-1α. VEGF and PlGF-mediated transcription of KCC3b and KCC4 involved hypoxia response element (HRE) motifs in their promoters, as demonstrated by promoter analysis, EMSA and ChiP. These results were corroborated *in vivo* by adenoviral-mediated overexpression of PlGF in normal mice, which led to increased expression of mKCC3 and mKCC4 in erythroid precursors. Our studies show that VEGF and PlGF regulate transcription of KCC3b and KCC4 in erythroid cells via activation of HIF-1α, independent of hypoxia. These studies provide novel therapeutic targets for regulation of cell volume in RBC precursors, and thus, amelioration of dehydration in RBCs in sickle cell disease.
Am. J. Hematol. 89:273–281, 2014.

Introduction

The potassium chloride cotransporters (KCCs) are members of the superfamily of cation-chloride cotransporters (SCL12) and mediate the coupled, electroneutral movement of K^+ and Cl^- ions across the plasma membrane. KCC proteins play important roles in the regulation of cell volume, ion homeostasis, and transepithelial ion transport [1]. Of the four mammalian members of this family [2,3], KCC1 is ubiquitously expressed [1], while KCC2 is found primarily in neuronal tissue [4]. KCC3 transcripts are abundant in the heart and kidney [5,6], and KCC4 is expressed in skeletal muscle, heart, liver, and brain [6,7]. KCC1, KCC3, and KCC4 proteins are expressed in both human and mouse RBCs, although levels are higher in reticulocytes [8]. In sickle cell disease (SCD), high KCC activity causes dehydration of reticulocytes, and higher intracellular hemoglobin concentration [9], increasing the rate of polymerization of HbSS thereby, contributing to sickling and the pathophysiology of SCD [10–12].

Clinical manifestations of SCD, include chronic hemolytic anemia, painful vascular occlusions and end-organ damage [13–15]. SCD patients and sickle mouse models exhibit increased circulatory levels of inflammatory cytochemokines, such as IL-8 [16] and TNF-α [17,18], as well as angiogenic factors, placental growth factor (PlGF) and vascular endothelial growth factor (VEGF) [19]. Less is known about the regulation of KCC gene expression in RBCs. In other cells, KCC3 and KCC4 expression has been shown to be regulated by insulin-like growth factor [20,21] platelet-derived growth factor (PGDF) [22] and VEGF [5]. Because VEGF and PlGF levels are elevated in sickle cell patients when compared with normal individuals [23], we hypothesized that these angiogenic factors also regulate KCC expression in erythroid cells. To address this hypothesis, we examined the effect of VEGF and PlGF on KCC expression in the erythroid cell line K562, using pharmacological and genetic approaches. Our findings provide evidence that angiogenic growth factor(s) regulate transcription of KCC transporters in erythroid cells via HIF-1α, independent of hypoxia.

Additional Supporting Information may be found in the online version of this article.

[1]Division of Hematology, Cancer and Blood Diseases Institute, Cincinnati Children's Hospital Medical Center, Cincinnati, Ohio; [2]Department of Biochemistry and Molecular Biology, Keck School of Medicine of the University of Southern California, Los Angeles, California; [3]Department of Pediatrics, Aflac Cancer and Blood Disorders Center, Emory University, Atlanta, Georgia

Conflict of interest: The authors report no conflicts of interest.
***Correspondence to:** Clinton H. Joiner, Division of Hematology/Oncology, Department of Pediatrics, Emory-Children's Center, Room 401, 2015 Uppergate Drive, Atlanta, GA 30030. E-mail: clinton.joiner@emory.edu
Contract grant sponsor: NIH; Contract grant number: U54 HL070871 (to CHJ).
Received for publication: 8 August 2013; **Revised:** 1 November 2013; **Accepted:** 11 November 2013
Am. J. Hematol. 89:273–281, 2014.
Published online: 14 November 2013 in Wiley Online Library (wileyonlinelibrary.com).
DOI: 10.1002/ajh.23631

Methods

Cell culture and reagents

K562, a human erythroid cell line obtained from American Type Cell Culture (Manasa, WA), was cultured in RPMI 1640 medium containing 10% heat inactivated fetal bovine serum. Unless otherwise indicated, K562 cells were kept overnight in serum-free medium, prior to treatment with human recombinant VEGF (250 ng/ml) or PlGF (250 ng/ml) (Peprotech, Rocky Hill, NJ), as previously described [24]. Diphenyliodonium chloride (DPI), LY294002, PD98059, SP600125, rapamycin, and SB203580 were obtained from Tocris Biosciences (Ellisville, MO). R59949 (diacyl glycerol kinase inhibitor) was purchased from Calbiochem (Gibbstown, NJ). Pharmacological inhibitors were dissolved in DMSO or water as per manufacturer's instructions. Inhibitors were used at concentrations that were deemed optimal from previous experiments and literature [25,26]. Primary antibodies for HIF-1α, β-actin, $p47^{phox}$, p38 MAP kinase, JNK, and secondary HRP-conjugated antibodies, siRNAs for p38 MAP kinase, $p47^{phox}$, JNK, PHD2, and HIF-1α, and the control siRNA were obtained from Santa Cruz Biotechnology (Santa Cruz, CA).

Luciferase reporter assays and transfections of siRNAs

Cells were transfected with 3 μg of the luciferase reporter construct, and 0.3 μg of a CMV β-galactosidase control plasmid, using the Transit LT-1 transfection reagent (Mirus, Madison, WI). Luciferase values were normalized to β-galactosidase values. Data are expressed relative to the activity of the promoter-less pGL3 basic vector. For RNAi experiments, K562 cells were transfected with 50 nM of the siRNAs or control siRNA, using the Transit LT-I transfection reagent.

RNA extraction and real-time qRT-PCR

Total mRNA for qRT-PCR was extracted using the RNAeasy micro kit (Qiagen, Valencia, CA). qRT-PCR assays for human and murine KCC mRNAs were run using TaqMan primers and probes [27]. Relative quantification (RQ) values for mRNA expression were calculated as $2^{-\Delta\Delta Ct}$ [28], where $\Delta\Delta Ct = (Ct$ target gene of treated sample $- Ct$ GAPDH of treated sample) – (Ct target gene of control sample $- Ct$ GAPDH of control sample).

Western blot analysis

Cells were lysed using an RIPA buffer [29]. Protein lysates were run on a 10% acrylamide gel. Membranes were stripped and re-probed with an antibody to β-actin (1:2,500) (Genscript, Piscataway, NJ), as a loading control. Bands were detected using the Supersignal West Pico detection kit (Pierce Biotechnology, Rockford, IL). Densitometric analysis was performed using ImageJ [30].

NanoPro assay

KCC1, KCC3a, KCC3b, KCC4, and ERK protein expression were measured by the NanoPro 1000 System (Protein Simple). In brief, the K562 cells were stimulated with human VEGF (250 ng/ml) or PlGF (250 ng/ml) for 24 hr lysed in lysis buffer (ProteinSimple). The lysates were centrifuged and loaded in small capillaries with Ampholyte premix G2 (ProteinSimple) and *pI* standard ladder 3. Isoelectric focusing of proteins was performed by applying 21,000 mW for 40 min, followed by treatment with UV light to cross-link proteins to the inner capillary wall. The capillary was washed and immunoprobed for the indicated proteins. The results were analyzed using the Compass® software. Peak area was generated using a total anti-KCC antibodies [27] and ERK antibody, representing KCC1, KCC3a, KCC3b, KCC4, and ERK isoforms. Using ERK as an internal control, the amount of KCC1, KCC3a, KCC3b, and KCC4 was determined by calculating the ratio between KCC isoform peak height and ERK peak height [31,32].

Electrophoretic mobility shift assay (EMSA) for transcription factor HIF-1α binding to HRE sites

Double-stranded oligonucleotide probes (Supporting Information Table 1) corresponding to the appropriate HRE sites in the KCC3b and KCC4 promoters were biotin labeled (Pierce Biotechnology/Thermo Scientific, Rockford, IL). EMSAs were run as previously described [26]. A 50-fold excess of unlabeled probe was used to demonstrate the specificity of the interaction between the protein and DNA. In supershift assays, nuclear extracts were preincubated for 30 min with HIF-1α antibody (2 μg), prior to addition of the labeled oligonucleotide.

KCC promoter luciferase reporter constructs

For the KCC3b luciferase construct, a fragment −1,100 to +142 bp from the transcription start site was PCR amplified using the human BAC clone CTD-2262M9 (Invitrogen/Life Technologies, Grand Island, NY) as a PCR template and inserted into the pXP2 luciferase vector. The −190/+142 bp KCC3b was amplified from the −1,100/+142 bp KCC3b construct. The −190/+142 bp KCC3b HRE mutants were generated utilizing the QuikChange Lightening (Stratagene/Agilent Technologies, Santa Clara, CA) mutagenesis kit. Nucleotide enumeration is based on Genbank entry BC098390.1.

The −875/+12 bp KCC4 wild-type sequence was amplified using BAC clone CTD-3165K9 as a PCR template and cloned into the pXP2 luciferase vector. The −96/+12 bp KCC4 and the −65/+12 bp KCC4 wt promoter construct were generated by digesting the −875/+12 bp KCC4 wt construct, followed by re-ligation. Mutations at the indicated HRE and SP-1 nucleotide binding sites within the −875/+12 bp and −96/+12 bp KCC4 wt vectors were generated using the Quikchange Lightening mutagenesis kit (Stratagene/Agilent Technologies, Santa Clara, CA). Nucleotide enumeration was based on Genbank entry NM_005135.2. All constructs were confirmed by DNA sequencing.

Chromatin immunoprecipitation (ChIP) assay

K562 cells in serum-free medium were treated with either VEGF (250 ng/ml) or PlGF (250 ng/ml). ChIP analysis was performed using a HIF-1α antibody (Santa Cruz Biotechnology, Santa Cruz, CA) [26]. DNA was subjected to PCR amplification for 30 cycles using the following conditions: 95°C for 45 sec, 63°C for 30 sec, 72°C for 120 sec, using primers listed in Supporting Information Table 1. The PCR products were run on a 2% agarose gel.

PlGF overexpressing mice

PlGF was overexpressed in C57Bl/6 mice by injecting an adenovirus vector encoding murine PlGF cDNA (ad-PlGF) and an analogous control adenovirus expressing GFP (ad-GFP) intravenously [33]. Mice were injected via tail-veins with either Ad-GFP or Ad-PlGF at 1×10^9 vector DNA particles/animal, and animals were bled after 5 weeks to determine plasma PlGF levels. PlGF levels were measured by ELISA (R&D Systems, Minneapolis, MN).

Sorting of murine bone marrow for various stages of erythroid maturation

Fresh bone marrow cells were isolated from the PlGF and GFP overexpressing mice, and immunostained with FITC-conjugated anti-CD44 and PECy7-conjugated Ter119 antibodies (BD Biosciences, San Jose, CA) [34]. Single cell suspensions were sorted using FACS VantageSE with a 70 μm nozzle (BD Biosciences, San Jose, CA). Cytospin slides were prepared by centrifugation at 500*g* for 5 min in a Cytospin® 4 cytocentrifuge, and counter-stained with Wright stain to assess erythroid differentiation in the sorted samples.

Statistical analysis

Data are presented as mean ± SD. Control and VEGF or PlGF-treated samples were compared using a Student's *t* test. One-way ANOVA, followed by Tukey–Kramer test were used for multiple comparisons using the Instat-2 Software (Graph Pad, San Diego, CA). $P < 0.05$ was considered statistically significant.

Results

VEGF and PlGF upregulate mRNA and protein expression of KCCs in erythroid cells.

Both VEGF (Fig. 1A,B and Supporting Information Fig. 1) and PlGF (Fig. 1C,D and Supporting Information Fig. 1) increased KCC mRNA and protein expression in the erythroid leukemia cell line K562. VEGF at a concentration of 250 ng/ml, as deemed optimal from previous experiments and literature [24], increased mRNA expression of the KCC1, KCC3 (both alternatively spliced forms a and b) and KCC4 isoforms, (Fig. 1A) after 8 hr of treatment. KCC protein levels in K562 lysates were measured using the isoelectric focusing-based NanoPro 1000 System, using isoform-specific KCC antibodies (Fig. 1B,D and Supporting Information Fig. 1). Figure 1B illustrates that 24 hr incubation of K562 cells with VEGF caused increased protein levels of KCC1, KCC3b by ∼34 and 105%, respectively. VEGF increased the levels of KCC4 protein by approximately sixfold, similar to the increase in mRNA levels. K562 cells treated with PlGF (250 ng/ml), also showed increased expression of KCC1, KCC3b and KCC4 mRNAs (Fig. 1A,C) at 4 hr. Notably, KCC3a mRNA expression was not affected by PlGF treatment of K562 cells (Fig. 1C), indicating a differential effect on induction of KCC3 expresssion by these two angiogenic factors. When compared with VEGF, PlGF induced similar increases in KCC1 and KCC3b protein levels, commensurate with

 doi:10.1002/ajh.23631

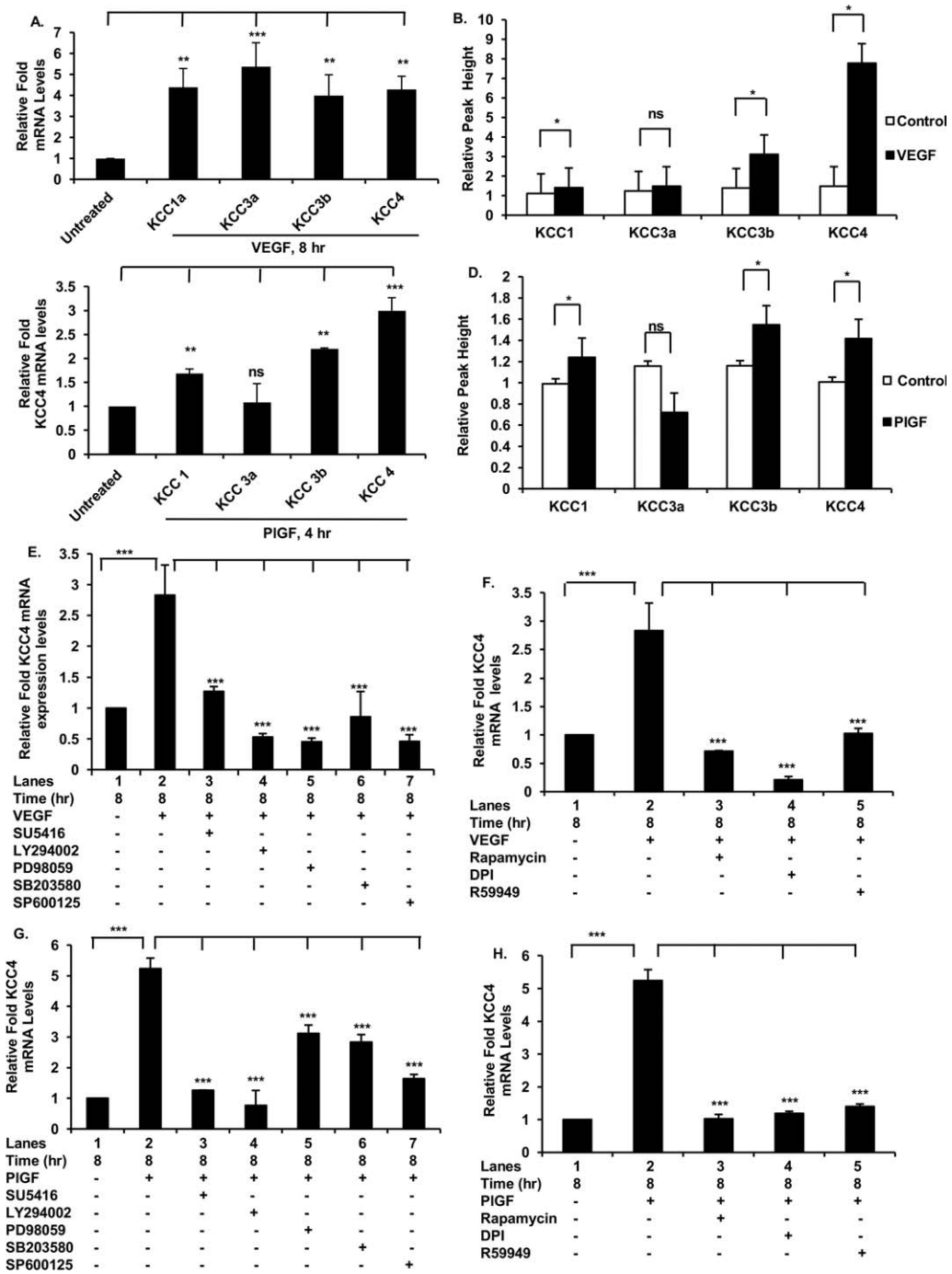

Figure 1. VEGF increases expression of the KCC genes in K562 cells: (A) VEGF-induced mRNA expression of the KCC isoforms in K562 cells after 8 hr of treatment. (B) VEGF induced protein expression of the KCC isoforms in K562 cells after 24 hr of treatment, using the NanoPro 1000 System as described in "Materials and Methods" and antibodies specific for KCC1, KCC3a, KCC3b KCC4, and anti-ERK as a loading control. Bar graph represents the ratio of the normalized signals in VEGF treated samples to control samples. (C) PlGF-induced expression of the KCC isoforms after 4 hr of treatment. (D) PlGF-induced expression of the KCC proteins in K562 cells (24 hr treatment). Bar graph represents the ratio of normalized signals in PlGF-treated samples to that of controls. (E,F) VEGF-induced and (G,H) PlGF-induced mRNA expression of KCC4, in K562 cells treated with the indicated pharmacological inhibitors (30 min). mRNA expression was normalized to GAPDH mRNA levels. Data are expressed as mean ± SD of three independent experiments. ***$P < 0.001$, **$P < 0.01$,*$P < 0.05$, ns, $P > 0.05$.

changes in mRNA levels for these isoforms (Fig. 1D and Supporting Information Fig. 1). KCC4 protein levels were also increased by PlGF, but to a lesser degree than mRNA levels and less than those seen with VEGF treatment (Fig. 1D and Supporting Information Fig. 1). These subtle differences in mRNA and protein expression responses to VEGF and PlGF suggest that post-transcriptional mechanisms, such as regulation by microRNAs [26], may be operative. Because a robust increase in the expression of KCC3b and KCC4 mRNA and protein levels was induced by both factors, we examined the mechanism governing their expression in erythroid cells.

VEGF and PlGF-mediated KCC4 expression in erythroid cells involves VEGFR-1

PlGF binds preferentially to VEGFR-1 (Flt-1), while VEGF binds to both VEGFR-1 and VEGFR-2 (Flk-1) in a variety of cells to

mediate intracellular signaling [35]. Although the VEGFR-1 receptor is expressed in megakaryocytic precursors [36] and K562 cells [37], the expression of these receptors in primary erythroid cells has not been delineated. Therefore, we determined the expression of VEGFR-1 and VEGFR-2 in erythroid precursor cells derived from bone marrow of normal mice (Supporting Information Fig. 2), isolated on the basis of CD44 expression and cell size (forward scatter) [34]. The VEGFR-1 receptor was expressed in early erythroblasts, with declining expression as maturation of erythroblasts progressed (Supporting Information Fig. 2). The expression of VEGFR-2 was not detectable in erythroblasts.

VEGF and PlGF-mediated upregulation of KCC4 involves VEGFR-1, PI-3kinase, MAP kinase, p38 MAP kinase, mTOR, NADPH-oxidase, and HIF-1α

To elucidate the signaling pathways involved in VEGF- and PlGF-mediated KCC4 expression, we utilized pharmacological inhibitors specific for various kinases. Pretreatment of K562 cells with a pharmacological inhibitor, SU5416 for VEGFR-1 and R-2 [38] significantly inhibited VEGF (Fig. 1E, lane 3 vs. lane 2) and PlGF-induced (Fig. 1G, lane 3 vs. lane 2) KCC4 expression, when compared with cells treated with VEGF or PlGF only. Inhibitors for PI3 kinase (LY294002), MAP kinase (PD98059), p38 MAP kinase (SB203580), and JNK (SP600125) inhibited VEGF-mediated KCC4 mRNA expression (Fig. 1E, lanes 4–7 vs. lane 2). DMSO, a solvent for inhibitors used, did not induce expression of KCC3b or KCC4 (data not shown). Significant inhibition of KCC4 mRNA levels was observed with the same inhibitors in PlGF treated cells (Fig. 1G, lanes 4–7 vs. lane 2). Mammalian target of rapamycin (mTOR) plays an important role in the PI-3 kinase/Akt pathway in VEGF-stimulated cancer cells [39]. As shown in Fig. 1F (lane 3) and Fig. 1H (lane 3) rapamycin attenuated KCC4 mRNA expression below the basal level, following treatment with either VEGF or PlGF. As reactive oxygen species (ROS), derived from nicotinamide adenine dinucleotide phosphate (NADPH)-oxidase, are also involved in VEGF- and PlGF-mediated cell signaling [40,41], we determined if these signaling pathways played a role in VEGF- and PlGF-mediated KCC3 and KCC4 expression in K562 cells. DPI, an inhibitor of NADPH-oxidase also attenuated KCC4 mRNA levels, in VEGF-treated cells (Fig. 1F, lanes 4 vs. lane 2) and in PlGF-treated cells (Fig. 1H, lane 4 vs. lane 2). The transcription factor, hypoxia-inducible factor-1α (HIF-1α) has been shown to play a role in PlGF-mediated gene expression of ET-1 and PAI-1 [25,33]. We found that R59949, which reduces levels of HIF-1α by simulating its degradation via prolyl hydroxylase-2 (PHD-2) [42], attenuated VEGF- and PlGF-mediated KCC4 mRNA expression to the basal level (Fig. 1F, lane 5, and Fig. 1H, lane 5). Thus, the data provide evidence that VEGF- and PlGF-mediated upregulation of KCC4 mRNA expression involved signaling through VEGF-R1 and downstream effectors PI-3kinase, MAP kinase, p38 MAP kinase, JNK, mTOR, NADPH-oxidase, and HIF-1α.

VEGF- and PlGF-mediated upregulation of KCC4 and KCC3b involves p38 MAP kinase, NADPH-oxidase and JNK

Since pharmacological inhibitors can have nonspecific or nontarget effects, we utilized siRNAs to knock-down specific kinases in the VEGF-R1 signaling pathway. VEGF-mediated KCC4 mRNA expression was reduced ~60, 75, and 110% by siRNAs for p38 MAP kinase, $p47^{phox}$ (a subunit of NADPH-oxidase) and JNK, respectively, as compared to scrambled (sc) control siRNA (Fig. 2A). We determined if the signaling pathways involved in VEGF-mediated expression of KCC4 also played a role in expression of KCC3b mRNA in response to VEGF. siRNAs for p38 MAP kinase, $p47^{phox}$, and JNK reduced VEGF-induced KCC3b mRNA levels to basal levels, when compared with cells transfected with a scrambled (sc) control siRNA (Fig. 2B). Efficient knockdown of JNK, p38 MAP kinase, and $p47^{phox}$ proteins was observed with the corresponding siRNAs (Supporting Information Fig. 3A–C). VEGF-dependent cellular signaling for KCC4 and KCC3b mRNA expression, therefore, involved p38 MAP kinase, NADPH-oxidase, and JNK.

VEGF-mediated upregulation of KCC3b and KCC4 involves activation of HIF-1α

SiRNA specific for HIF-1α reduced VEGF-induced mRNA expression of both KCC4 and KCC3b to basal levels (Fig. 2C,D, lane 4). PHD2 causes hydroxylation of proline residues in HIF-1α under normoxic conditions, marking it for ubiquitin-mediated degradation [43]. In the absence of VEGF, siRNA for PHD2 increased the expression of both KCC4 (Fig. 2C, lane 5 vs. lane 1) and KCC3b mRNA (Fig. 2D, lane 5 vs. lane 1) by approximately threefold, when compared with the untreated K562 cells. A nonspecific siRNA (scRNA), transfected as a control, had no effect on KCC4 (Fig. 2C, lane 3) and KCC3b (Fig. 2D, lane 3) mRNA levels. Western blot analysis confirmed the knockdown of HIF-1α (Supporting Information Fig. 3D, Fig. 2E, lane 4 vs. lane 2) and PHD2 (Supporting Information Fig. 3E, lane 4 vs. lane 2) proteins by their specific siRNAs, whereas nonspecific scrambled siRNAs (scRNAs) had no effect on protein levels. These findings are consistent with a role for HIF-1α in the regulation of KCC3b and KCC4 gene expression, and as a mediator of upregulation of these genes by VEGF.

VEGF stabilizes HIF-1α protein under normoxic conditions in K562 cells

Previous studies have shown that hypoxia causes the stabilization of HIF-1α, while normoxia brings about its degradation [43]. Recent studies suggest that HIF-1α can be stabilized independent of hypoxia by factors, such as ET-1 [26] or PlGF [44]. The treatment of K562 cells with VEGF increased levels of HIF-1α protein when compared with levels in untreated cells as determined by Western blots (Fig. 2E, lane 2 vs. lane 1). This increase in VEGF-mediated HIF-1α protein levels was inhibited to basal levels by the PI3 kinase inhibitor (LY294002) and the MAP kinase inhibitor (PD98059) (Fig. 2E, lanes 3 and 4 vs. lane 2). Moreover, SU5416, a VEGFR-1 receptor inhibitor [38] (Fig. 2E, lane 5 vs. lane 2) and R59949, a putative inhibitor of HIF-1α, also attenuated HIF-1α protein levels (Fig. 2E, lane 6). These data demonstrate that VEGF stabilizes HIF-1α protein in erythroid cells, independent of hypoxia via signaling involving VEGF-R1, PI-3 kinase, and MAP kinase.

Transcriptional activation of KCC4 mRNA expression involves selective HRE-sites and SP-1 cis-binding elements in its promoter

The HIF complex is known to modulate gene transcription by binding to promoter elements known as hypoxia response elements or HREs (RCGTG) [45]. *In silico* analysis of the KCC4 promoter region revealed the presence of two HREs at positions −21 to −18 bp (CCGTG) and −75 to −73 bp (ACGTG), relative to transcriptional start site (Fig. 3A). Two canonical SP-1 consensus sites are also present in the promoter at positions −44 to −35 and −64 to −56 bp. Luciferase assays of K562 cells transfected with the full length −875/+12 bp KCC4 promoter reporter construct and a truncated −96/+12 bp KCC4 promoter reporter construct yielded similar activity (Fig. 3B), indicating that the truncated promoter of KCC4 was sufficient for transcriptional activity. Further truncation of the

 doi:10.1002/ajh.23631

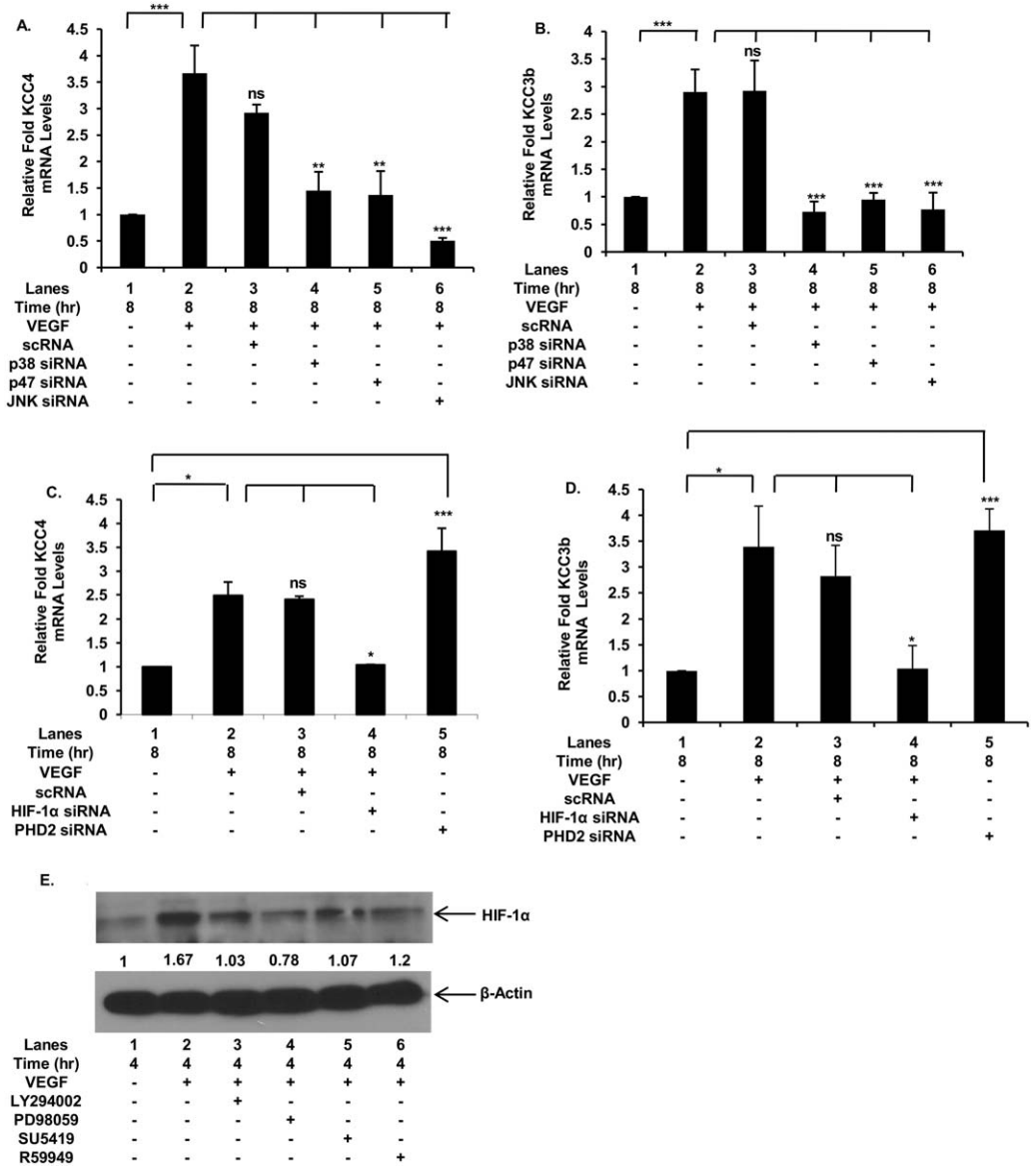

Figure 2. VEGF-induced KCC4 and KCC3b mRNA expression in K562 cells: K562 cells were transfected with siRNA for p38 MAP kinase, $p47^{phox}$, JNK kinase, and scrambled scRNA control, prior to stimulation with VEGF for 8 hr. (A) Effect of VEGF on KCC4 mRNA levels. (B) Effect of VEGF on KCC3b mRNA levels. (C,D) Effect of knock-down and overexpression of HIF-1α on KCC4 and KCC3b mRNA levels. Data is represented as mean ± SD of three, independent experiments. Data are expressed as mean ± SD of three independent experiments. $^{***}P < 0.001$, $^{**}P < 0.01$,$^{*}P < 0.05$, ns, $P > 0.05$. (E) VEGF treatment (8 hr) increases HIF-1α protein expression in K562 cells, which is attenuated by pharmacological inhibitors for PI3-kinase (LY294002), MAP kinase (PD98059), VEGF-R1 (SU5416), and HIF-1α (R59949). Western blots for HIF-1α were performed as described in "Materials and Methods". Blots were stripped and probed with β-actin to confirm equal loading. Data are representative of three independent experiments.

promoter construct to −65/−12 bp, eliminating the HRE site at position −76/−73 bp, showed reduced luciferase activity by ∼75% (Fig. 3B, lane 3). These data identify the −96/+12 bp region as the minimal promoter essential for transcription of KCC4 mRNA. Next, we created mutations of the individual HRE sites, designated as HRE 1m (at −21/−18 bp) and HRE 2m (at −76/−73 bp) within the full length −875/+12 bp of KCC4 promoter. The HRE1 mutant retained full promoter activity when compared with the full length −875/+12 bp KCC4 promoter (Fig. 3C, lane 2 vs. lane 1). However, mutation of the HRE2 *cis*-binding site led to ∼75% decrease in reporter activity (Fig. 3C, lane 3). Using the −96/+12 bp promoter construct, we also examined the role of SP-1 binding sites at positions −44 to −35 and −64 to −56 bp in transcription of KCC4 mRNA. Mutations at either of these SP-1 binding sites substantially (∼90%) reduced KCC4 promoter activity, when compared with the −96/+12 bp KCC4 promoter (Fig. 3C, lanes 5 and 6 vs. lane 4) construct. Taken together, the data showed that the HRE site at −75/−73 bp (HRE2), but not the HRE site at −21/−18 bp (HRE1), and both SP-1 sites were involved in regulating KCC4 mRNA expression at basal levels.

Transcriptional activation of KCC3b mRNA expression involves HRE-sites in its promoter

In silico analysis of the KCC3b proximal promoter region showed two HRE sites at positions −9 bp to −6 bp (HRE1, ACGTG) and −49 to −46 bp (HRE2, GCGTG) relative to transcriptional start site, as depicted in Fig. 3D. K562 cells transfected with a −190/+142 bp KCC3b promoter luciferase construct showed similar levels of luciferase activity as compared to the full length −1,100/+142 bp KCC3b luciferase promoter construct (Fig. 3E, lane 2 vs. lane 1), suggesting

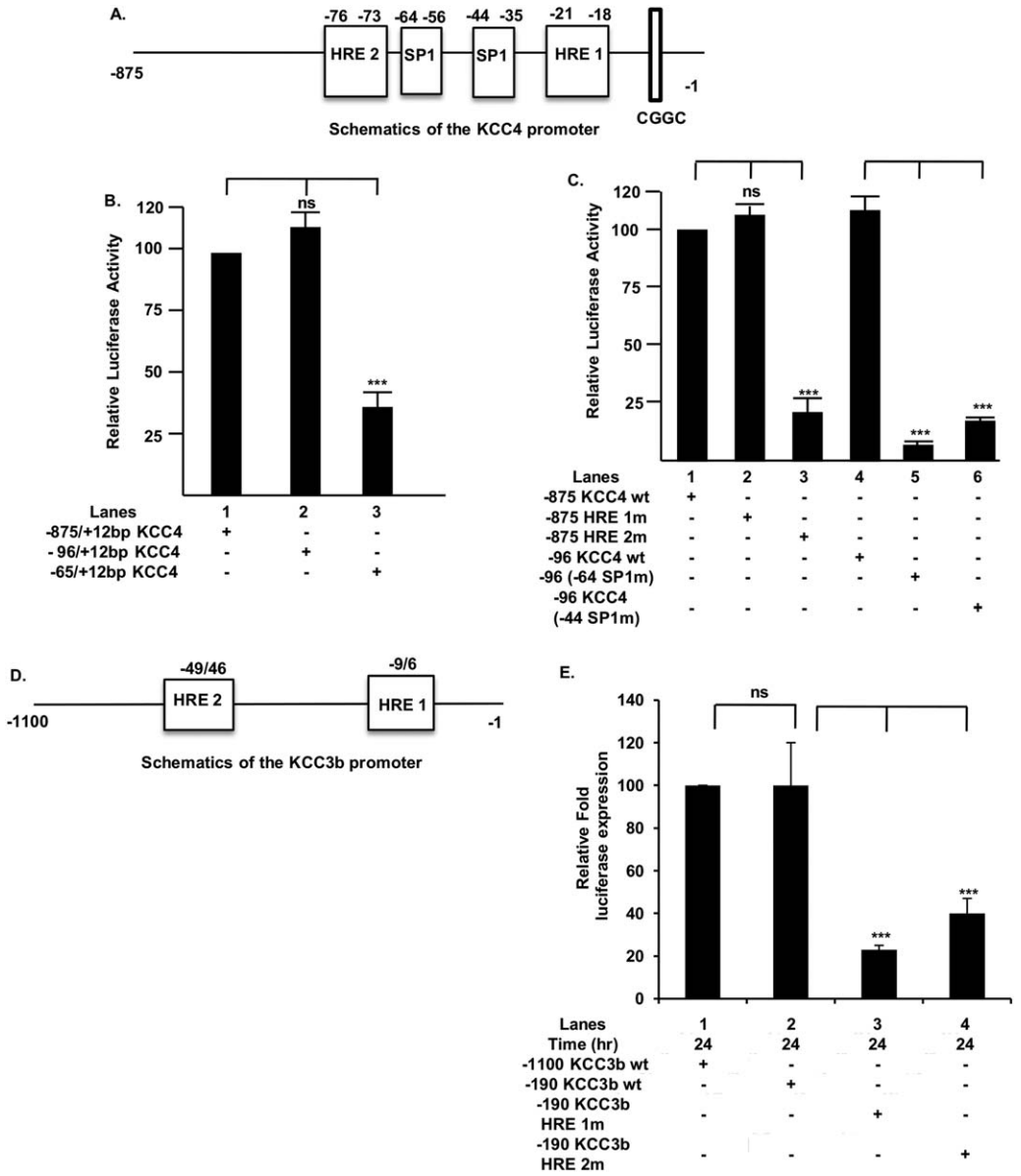

Figure 3. KCC4 and KCC3b promoter activity requires the activity of HIF-1α. (A) Schematic of the KCC4 (−875/+12 bp) promoter region, containing two HRE sites and two SP-1 binding sites. (B) Deletion analysis of KCC4 promoter utilizing reporter luciferase assay. (C) Analysis of HRE and SP-1 binding sites in the KCC4 promoter. (D) Schematic of the KCC3b (−1,100/+142 bp) promoter region containing two HRE sites. (E) Promoter analysis of the KCC3b (−1,100/+142 bp) promoter by reporter luciferase assay. Data are mean ± SD of three independent experiments. ***$P < 0.001$, **$P < 0.01$, *$P < 0.05$, ns $P > 0.05$.

that the −190/+142 bp promoter regions is the minimal region required for KCC3b promoter activity. Mutations within the HRE1 site at positions −9/−6 bp of the −190/+142 bp KCC3b promoter construct led to ∼90% decrease in reporter luciferase activity, when compared with the −190/+142 bp KCC3b construct (Fig. 3E, lane 3 vs. lane 2). In addition, mutation of the HRE2 site at position −49/−46 bp reduced reporter luciferase activity by ∼80% (Fig. 3E, lane 4). Taken together, these results showed that both HRE sites within the KCC3b promoter were required for KCC3b mRNA expression at basal levels.

VEGF augments binding of HIF-1α *in vitro* (EMSA) and *in vivo* (ChIP) to the promoter regions of KCC4

In an electrophoretic mobility shift assay (EMSA), using an oligonucleotide probe spanning the HRE2 site at −76/−73 bp of the KCC4 promoter, VEGF treatment of K562 cells showed increased probe binding to nuclear extracts (Supporting Information Fig.4A, lane 2 [1.5 ± 0.16] vs. lane 1). An oligonucleotide probe with mutations in the HRE site (Table 1) resulted in reduced binding of (Supporting Information Fig. 4A, lane 3 [0.89 ± 0.13] vs. lane 2). A 50-fold excess of the unlabeled probe competed out biotin-labeled probe binding (Supporting Information Fig. 4A, lane 4 [0.95 ± 0.13] vs. lane 2), and antibody to HIF-1α reduced binding to the wild-type oligonucleotide probe (Supporting Information Fig. 4A, lane 5 [1.09 ± 0.18] vs. lane 2).

To determine whether HIF-1α binds to the KCC4 promoter, we performed chromatin immunoprecipitation (ChIP) assays. VEGF treatment of K562 cells showed increased binding of HIF-1α to the KCC4 promoter in native chromatin (Fig. 4A, top panel) as reflected by the increase in the expected 200 bp PCR product corresponding to the KCC4 promoter region containing the HRE site at position −76/−73 bp. Immunoprecipitation with control rabbit IgG did not display any significant amplification of the expected PCR products (Fig. 4A, middle

 doi:10.1002/ajh.23631

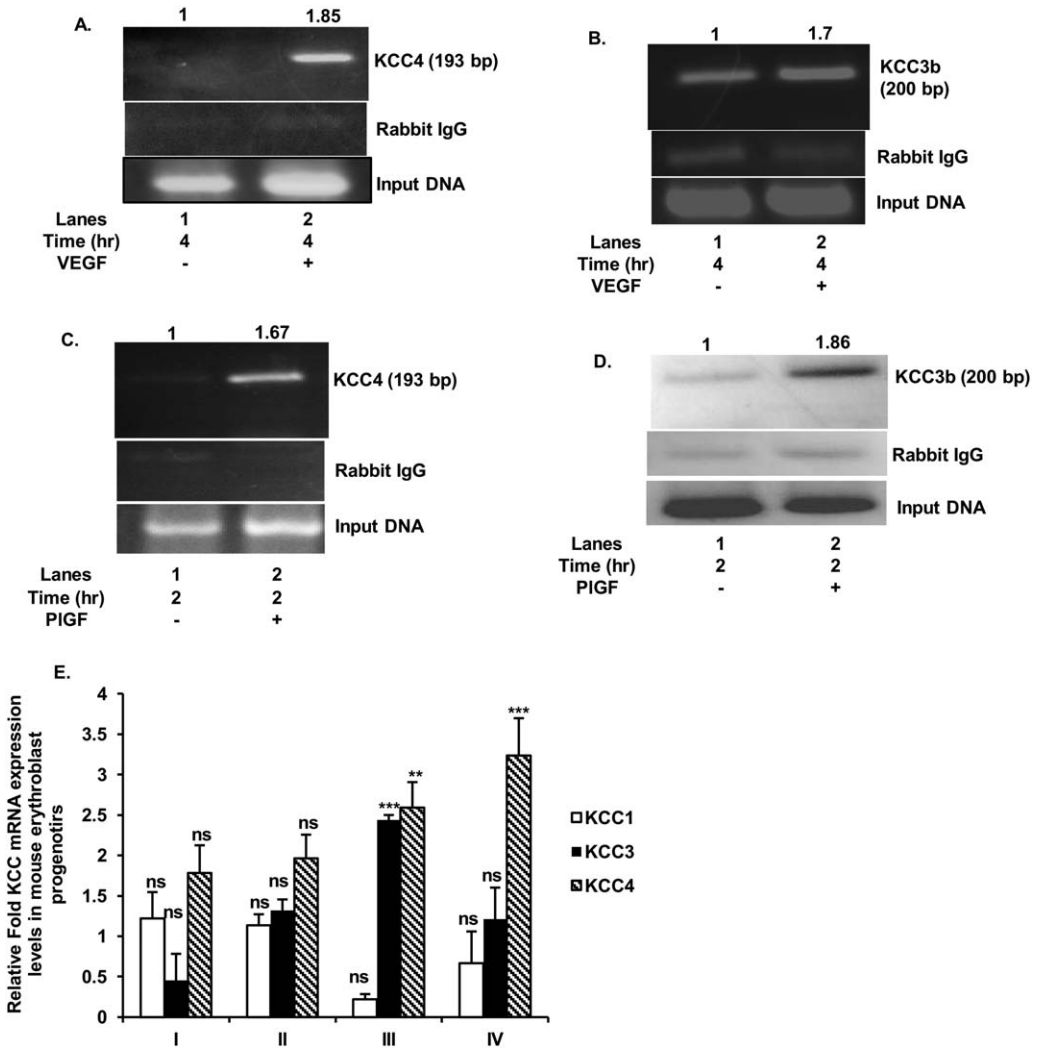

Figure 4. VEGF and PlGF induce binding of HIF-1α to the KCC4 and KCC3b promoters in K562 cells. (A,B) ChIP analysis of HIF-1α binding to the KCC4 and KCC3b promoter in K562 cells treated without and with VEGF for 4 hr. (C,D) ChIP analysis of the KCC4 and KCC3b promoter in K562 cells treated with PlGF. HIF-1α antibody (top panel) or control rabbit IgG (middle panel) was used for immunoprecipitation of soluble chromatin. The bottom panel represents the amplification of input DNA before immunoprecipitation. Primers used to amplify the PCR products are indicated in Supporting Information Table 1. Data are representative of three independent experiments. (E) Ter199^{+} bone marrow progenitors were sorted by flow cytometry based on CD44 expression and forward scatter into I: Proerythroblast and basophilic normoblasts, II: Basophilic and polychromatophilic normoblasts, III: Polychromatophilic and orthochromatic normoblasts, and IV: Orthochromatic normoblasts, reticulocytes, and RBCs (Supporting Information Fig. 1A). KCC mRNA expression, as determined by qRT-PCR, was normalized to corresponding GAPDH mRNA levels. qRT-PCR data from cells from PlGF overexpressing mice were further normalized to values obtained from control mice overexpressing GFP, to yield fold-changes in KCC mRNA expression. Data are expressed as mean ± SD of three independent experiments. ***$P < 0.001$, **$P < 0.01$, *$P < 0.05$, ns, $P > 0.05$

panel). Amplification of the PCR products as input DNA, before immunoprecipitation with the HIF-1α antibody, was similar in both samples (Fig. 4A, bottom panel). Taken together, the data showed HIF-1α binds to native chromatin to up-regulate the KCC4 expression *in vivo*.

VEGF augments binding of HIF-*1α* in-vitro (EMSA) and in-vivo (ChIP) to the promoter regions of KCC3b

Nuclear extracts from VEGF-treated K562 cells showed increased binding to an oligonucleotide probe spanning the HRE site at −9/−6 bp (HRE1) of the KCC3b promoter (Supporting Information Fig. 4B, lane 2 [1.51 ± 0.13] vs. lane 1), as determined by EMSA. A 50-fold excess of unlabeled probe competed out HIF-1α binding in nuclear extracts (Supporting Information Fig. 4B, lane 3 [0.9 ± 0.08]). An oligonucleotide with mutations within the HRE site abrogated binding of nuclear extract (Supporting Information Fig. 4B, lane 4 [0.91 ± 0.18]). Incubation of nuclear extracts with a HIF-1α antibody also reduced binding of the HIF-1α protein to the −9/−6 bp HRE site in the KCC3b promoter (Supporting Information Fig. 4B, lane 5 [0.97 ± 0.09] vs. lane 2). The oligonucleotide probe spanning the HRE site at −49/−46 bp (HRE2) in KCC3b promoter also showed increased binding to nuclear extracts from VEGF-treated K562 cells (Supporting Information Fig. 4C, lane 2 [1.5 ± 0.04] vs. lane 1). Probe binding to the nuclear extracts of VEGF-treated cells was reduced by addition of 50-fold excess of unlabeled probe (Supporting Information Fig. 4C, lane 3 [1.00 ± 0.20]), as well as by mutation of the HRE motif (Supporting Information Fig. 4C, lane 4 [0.95 ± 0.12]), and by the addition of a HIF-1α antibody (Supporting Information Fig. 4C, lane 5 [1.17 ± 0.08]).

The results of EMSA analysis were corroborated by ChIP analysis using an HIF-1α antibody and PCR primers specific for the KCC3b promoter region encompassing both the HRE sites at −9/−6 bp (HRE1) and −49/−46 bp (HRE2) (Fig. 4B, top panel). Untreated cells showed some occupation of the promoter by HIF-1α, which was increased by VEGF treatment (Fig. 4B). Immunoprecipitation with

control rabbit IgG did not show substantial amplification of the expected PCR products (Fig. 4B, middle panel). Amplification of the PCR products, prior to immunoprecipitation with HIF-1α antibody, confirmed similar amount of input DNA, in untreated and VEGF-treated samples from K562 cells (Fig. 4B, bottom panel). Thus, both HRE sites in KCC3 promoter appear to be involved in VEGF-mediated transcription of KCC3b *in vitro* and *in vivo*.

PlGF augments binding of HIF-1α *in vivo* to the promoter regions of KCC4 and KCC3b

ChIP analysis of chromatin samples derived from PlGF-treated cells immunoprecipitated with HIF-1α antibody showed approximately a twofold increase in the expected PCR product of 193 bp size, corresponding to the KCC4 promoter region spanning the HRE site at −76/−73 bp (HRE2) as compared to control, untreated cells (Fig. 4C, top panel). Immunoprecipitation of chromatin samples with normal rabbit IgG showed no amplification of the PCR product (Fig. 4C, middle panel), and loading of the input DNA was similar in both lanes (Fig. 4C, bottom panel).

ChIP analysis of the KCC3b promoter also showed approximately two-fold increase in the amplification of the expected PCR product (200 bp) spanning both HRE sites within the promoter (Fig. 4D, top panel), in PlGF-treated cells. Immunoprecipitation with a control rabbit IgG showed minimal amplification of the PCR product (Fig. 4D, middle panel), and input DNA controls were comparable (Fig. 4D, bottom panel). These results indicate that HIF-1α binds to both the KCC3b and KCC4 promoter in native chromatin of K562 cells when treated with PlGF.

Overexpression of PlGF *in vivo* augments expression of the KCC3 and KCC4 isoforms in mouse erythroblast progenitors

In silico analysis revealed that the HRE sequences within the KCC3b and KCC4 promoters are conserved in mice and humans; thus, we examined whether PlGF regulated the expression of KCC3 and KCC4 mRNA in mouse erythroid cells *in vivo*. To analyze the effect of PlGF on KCC expression *in vivo*, we overexpressed PlGF in C57BL/6 mice by intravenous injection with an adenoviral vector coding for PlGF, whereas the control mice received a vector encoding GFP [33]. PlGF expression was sustained, with levels in treated animals ranging from 300 to 391 pg/ml (mean = 338 ± 27 pg/ml) as compared to levels of 5–8 pg/ml (mean = 8 ± 2 pg/ml) in control GFP animals. After 4 weeks of vector injection, erythroid subpopulations at progressive stages of differentiation were isolated from the marrow of four mice overexpressing PlGF and control mice, utilizing flow cytometry and gating on Ter-119-positive erythroid cells, and sorting on the basis of CD44 staining and forward scatter [34]. Proportions of the sorted population were quantified by cytospins; thus, confirming the progression of erythroid differentiation from population stages I–IV (Fig. 4E). The effect of PlGF overexpression on KCC mRNA levels by quantitative PCR was expressed as the ratio of KCC mRNA levels in isolated erythroid fractions derived from PlGF-mice to that of the GFP-injected mice. As shown in Fig. 4E, the KCC4 mRNA levels were significantly increased in polychromatophilic and orthochromatic erythroblasts (stage III), as well as in reticulocytes (stage IV), but not in earlier precursors (proerythroblast and basophilic erythroblasts (stage I) and basophilic and polychromatophilic erythroblasts (stage II) in PlGF-overexpressing mice. KCC3 mRNA, which is the principle KCC species in mouse erythroblasts [27] was increased ∼2.5-fold only in population III containing polychromatophilic and orthochromatic normoblasts (Fig. 4E). The expression of KCC1 was not changed significantly in any of the erythroblast populations. These data showed that elevation of PlGF levels in vivo resulted in increased expression of KCC3 and KCC4 mRNAs in erythroid precursors in mid to late phases of erythroid differentiation.

Discussion

In this study, we provide evidence that VEGF and PlGF increase the transcription of KCC genes in erythroid cells via hypoxia-independent stabilization of HIF-1α protein. VEGFR-1 was expressed in erythroid K562 cells and early erythroid precursors *in vivo*. VEGFR-1 blockade significantly reduced VEGF and PlGF stimulation of KCC expression in K562 cells. The stimulatory patterns of KCC expression in VEGF and PlGF were subtly different: both increased message levels for KCC1, KCC3b, and KCC4, but only VEGF also increased KCC3a mRNA levels. Protein levels of KCC1, KCC3b, and KCC4 were increased in K562 cells by both VEGF and PlGF. Using pharmacologic approaches confirmed by RNA interference, we showed that the canonical PI-3 kinase pathways activated by VEGFR-1, involving p38 MAP kinase, NADPH-oxidase, mTOR, and JNK kinase, was responsible for VEGF/PlGF upregulation of KCC expression. VEGF and PlGF stabilized HIF-1α levels in K562 cells [25,33], and manipulation of HIF-1α modulated VEGF stimulation of KCC expression. The *cis*-acting regulatory elements (hypoxia responsive elements or HREs) which mediate HIF-1α transcriptional regulation [46] were present at multiple sites in the promoter regions of the all three KCC genes. Detailed analysis of the KCC3b and KCC4 promoters demonstrated functional activity of several of these HREs, as well as the binding motifs for SP-1 transcription factor. *In vitro* and *in vivo* binding of HIF-1α to HRE sites was augmented by VEGF and PlGF as demonstrated by EMSA and ChIP assays. Finally, in mice induced to overexpress PlGF, KCC expression in erythroid precursors was upregulated compared to cells from control mice. These data constitute a consistent and compelling body of evidence to support the notion that the angiogenic factors, VEGF and PlGF, acting through VEGF R-1 upregulate transcription of KCC transporters in erythroid cells via a HIF-1α-dependent, hypoxia-independent mechanism.

Our findings corroborate and extend previous studies on the transcriptional regulation of KCC genes by factors such as insulin-like growth factor (IGF-1) and platelet-derived growth factor (PDGF) [5,20,22]. Both, IGF-1 and PDGF signal through receptors linked to PI-3 kinase and its downstream regulators to increase HIF-1α levels [47]. VEGF and PlGF-mediated signaling through VEGF R-1 has been shown to result in hypoxia-independent activation of HIF-1α and in HIF-1α-dependent increase of several other genes in different cell types [24,44]. PlGF and VEGF are elaborated from erythroid precursors, but not by other hematopoietic cells [48–50]. Under conditions of erythroid hyperplasia, such as SCD and other hemolytic anemia, levels of VEGF and PlGF are high in plasma [19,49,50]. The pathophysiological importance of the elevation of these angiogenic growth factors is accentuated by findings that cytochemokines (e.g. IL-1α, IL-8, MCP-1, and MIP-1β) are elevated in the plasma of sickle cell patients and are upregulated by PlGF treatment of normal cells [16–18,51]. These findings support a central role of angiogenic factors in driving the proinflammatory and procoagulant vasculopathy that characterizes SCD.

The production of VEGF/PlGF by erythroblasts and the regulation of gene expression of KCC and perhaps other HIF-1α-dependent genes in these cells represents an autocrine/paracrine phenomenon that could be magnified by erythropoietic stress in SCD and other hemolytic conditions. It remains to be determined whether perturbations of KCC expression by elevated levels of VEGF/PlGF in SCD result in altered KCC protein content and/or function in sickle reticulocytes that could explain the dysregulation of the volume regulatory behavior of the KCC system in these cells. Based on our findings, it is conceivable that erythroid differentiation under high VEGF/PlGF stimulation could result in cells with altered contents or ratios of KCC proteins. Indeed, we have demonstrated that the ratio of KCC1

 doi:10.1002/ajh.23631

protein to KCC3 is higher in SS RBC membranes than AA RBC [27]. VEGF/PlGF-stimulated changes in KCC gene expression may increase KCC activity in a way that fosters RBC dehydration and thus hemolysis; thereby, amplifying the pathology of SCD.

The present study illuminates novel mechanisms of transcriptional regulation of KCC proteins in erythroid cells, and their alteration by the abnormal cytokine milieu in SCD. Our findings rise the possibility that altering or interfering with the angiogenic cytokines, VEGF and PlGF, and their downstream effectors might not only mitigate the proinflammatory and procoagulant state of SCD but also improve the functional behavior of sickle red blood cells.

Author Contributions

C.H.J. was the principal investigator and takes responsibility for the paper. C.S.G., S.C., S.C., and W.L. performed the experiments. C.S.G., C.H.J., and V.K. analyzed data and wrote the paper.

Acknowledgment

The authors thank Punam Malik (Cincinnati Children's Hospital Medical Center) for kindly providing PlGF-overexpressing mice. CSG was a Sickle Cell Research Scholar.

References

1. Gamba G. Molecular physiology and pathophysiology of electroneutral cation-chloride cotransporters. Physiol Rev 2005;85:423–493.
2. Lauf PK, Adragna NC. K–Cl cotransport: Properties and molecular mechanism. Cell Physiol Biochem 2000;10:341–354.
3. Mount DB, Gamba G. Renal potassium–chloride cotransporters. Curr Opin Nephrol Hypertens 2001;10:685–691.
4. Payne JA, Stevenson TJ, Donaldson LF. Cloning and expression of a neuronal-specific K–Cl cotransporter in rat brain. Soc Neurosci Abstr 1996;22:732.
5. Hiki K, D'Andrea RJ, Furze J, et al. Cloning, characterization, and chromosomal location of a novel human K+–Cl− cotransporter. J Biol Chem 1999;274:10661–10667.
6. Mount DB, Mercado A, Song LY, et al. Cloning and characterization of KCC3 and KCC4, new members of the cation-chloride cotransporter gene family. J Biol Chem 1999;274:16355–16362.
7. Boettger T, Hubner CA, Maier H, et al. Deafness and renal tubular acidosis in mice lacking the K–Cl co-transporter Kcc4. Nature 2002;416:874–878.
8. Crable SC, Hammond SM, Papes R, et al. Multiple isoforms of the KC1 cotransporter are expressed in sickle and normal erythroid cells. Exp Hematol 2005;33:624–631.
9. Quarmyne M, Risinger M, Linkugel A, Frazier A, Joiner, C. Defining a phenotype for red cell volume regulation and potassium chloride cotransport. Blood Cells Mol Dis 2011;47:95–99.
10. Brugnara C. Sickle cell disease: From membrane pathophysiology to novel therapies for prevention of erythrocyte dehydration. J Pediatr Hematol Oncol 2003;25(12):927–933.
11. Nagel RL, Fabry ME, Steinberg MH. The paradox of hemoglobin SC disease. Blood Rev 2003; 17(3):167–178.
12. Rinehart J, Gulcicek EE, Joiner CH, et al. Determinants of erythrocyte hydration. Curr Opin Hematol 2010;17(3):191–197.
13. Francis RB, Johnson CS. Vascular occlusion in sickle-cell disease:current concepts and unanswered questions. Blood 1991;77:1405–1414.
14. Platt OS, Thorington BD, Brambilla DJ, et al. Pain in sickle-cell disease—rates and risk-factors. New Engl J Med 1991;325:11–16.
15. Embury SH, Hebbel RP, Mohandas N, et al. Pathogenesis of vasoocclusion. In: Sickle Cell Disease: Basic Principles and Clinical Practice, Embury SH, Hebbel RP, Mohandas N, Steinberg MH (Eds), Raven Press, New York 1994. p. 311.
16. Duits AJ, Schnog JB, Lard LR, et al. Elevated IL-8 levels during sickle cell crisis. Eur J Haematol 1998;61:302–305.
17. Francis RB, Haywood LJ. Elevated immunoreactive tumor-necrosis-factor and interleukin-1 in sickle-cell-disease. J Natl Med Assoc 1992;84:611–615.
18. Croizat H, Nagel RL. Circulating cytokines response and the level of erythropoiesis in sickle cell anemia. Am J Hematol 1999;60:105–115.
19. Sundaram N, Tailor A, Mendelsohn L, et al. High levels of placenta growth factor in sickle cell disease promote pulmonary hypertension. Blood 2010;116(1):109–112.
20. Shen MR, Lin AC, Hsu YM, et al. Insulin-like growth factor 1 stimulates KCl cotransport, which is necessary for invasion and proliferation of cervical cancer and ovarian cancer cells. J Biol Chem 2004;279:40017–40025.
21. Di Fulvio M, Lincoln TM, Lauf PK, et al. Protein kinase G regulates potassium chloride cotransporter-3 expression in primary cultures of rat vascular smooth muscle cells. J Biol Chem 2001;276:21046–21052.
22. Zhang J, Lauf PK, Adragna NC. PDGF activates K–Cl cotransport through phosphoinositide 3-kinase and protein phosphatase-1 in primary cultures of vascular smooth muscle cells. Life Sci 2005;77:953–965.
23. Gurkan E, Tanriverdi K, Baslamish F. Clinical relevance of vascular endothelial growth factor levels in sickle cell disease. Ann Hematol 2005; 84:71–75.
24. Selvaraj SK, Giri RK, Perelman N, et al. Mechanism of monocyte activation and expression of proinflammatory cytochemokines by placenta growth factor. Blood 2003;102:1515–1524.
25. Patel N, Gonsalves CS, Malik P, et al. Placenta growth factor augments endothelin-1 and endothelin-B receptor expression via hypoxia-inducible factor-1 alpha. Blood 2008;112:856–865.
26. Gonsalves C, Kalra VK. Endothelin-1-induced macrophage inflammatory protein-1 beta expression in monocytic cells involves hypoxia-inducible factor-1 alpha and AP-1 and is negatively regulated by microRNA-195. J Immunol 2010;185:6253–6264.
27. Pan D, Kalfa TA, Wang D, et al. K–Cl cotransporter gene expression during human and murine erythroid differentiation. J Biol Chem 2011;286:30492–30503.
28. Pfaffl MW. A new mathematical model for relative quantification in real-time RT-PCR. Nucleic Acids Res 2001;29(9):e45.
29. Kim KS, Rajagopal V, Gonsalves C, et al. A novel role of hypoxia-inducible factor in cobalt chloride- and hypoxia-mediated expression of IL-8 chemokine in human endothelial cells. J Immunol 2006;177:7211–7224.
30. Schneider CA, Rasband WS, Eliceiri KW. NIH Image to ImageJ: 25 years of image analysis. Nature Methods 2012;9:671–675.
31. de Kreuk B-J, Anthony EC, Geerts D, et al. The F-BAR protein PACSIN2 regulates epidermal growth factor receptor internalization. J Biol Chem 2012;287:43438–43453.
32. Xin H-W, Ambe CM, Hari DM, et al. Label-retaining liver cancer cells are relatively resistant to sorafenib. Gut 2013;00:1–10.
33. Patel N, Sundaram N, Yang MY, et al. Placenta growth factor (PlGF), a novel inducer of plasminogen activator inhibitor-1 (PAI-1) in sickle cell disease (SCD). J Biol Chem 2010;285:16713–16722.
34. Chen K, Liu J, Heck S, et al. Resolving the distinct stages in erythroid differentiation based on dynamic changes in membrane protein expression during erythropoiesis. Proc Natl Acad Sci USA 2009;106:17413–17418.
35. Clauss M, Weich H, Breier G, et al. The vascular endothelial growth factor receptor Flt-1 mediates biological activities: Implications for a functional role of placenta growth factor in monocyte activation and chemotaxis. J Biol Chem 1996;271:17629–17634.
36. Casella I, Feccia T, Chelucci C, et al. Autocrine-paracrine VEGF loops potentiate the maturation of megakaryocytic precursors through Flt1 receptor. Blood 2003;101:1316–1323.
37. Bellamy WT, Richter L, Frutiger Y, et al. Expression of vascular endothelial growth factor and its receptors in hematopoietic malignancies. Cancer Res 1999;59:728–733.
38. Itokawa T, Nokihara H, Nishioka Y, et al. Antiangiogenic effect by SU5416 is partly attributable to inhibition of FIt-1 receptor signaling. Mol Cancer Ther 2002;1:295–302.
39. Riesterer O, Zingg D, Hummerjohann J, et al. Degradation of PKB/Akt protein by inhibition of the VEGF receptor/mTOR pathway in endothelial cells. Oncogene 2004;23:4624–4635.
40. Ushio-Fukai M. VEGF signaling through NADPH oxidase-derived ROS. Antioxidants Redox Signal 2007;9:731–739.
41. Ushio-Fukai M, Nakamura Y. Reactive oxygen species and angiogenesis: NADPH oxidase as target for cancer therapy. Cancer Lett 2008;266:37–52.
42. Temes E, Martin-Puig S, Acosta-Iborra B, et al. Activation of HIF-prolyl hydroxylases by R59949, an inhibitor of the diacylglycerol kinase. J Biol Chem 2005;280:24238–24244.
43. Semenza GL. Signal transduction to hypoxia-inducible factor 1. Biochem Pharmacol 2002;64:993–998.
44. Patel N, Gonsalves CS, Yang MY, et al. Placenta growth factor induces 5-lipoxygenase-activating protein to increase leukotriene formation in sickle cell disease. Blood 2009;113:1129–1138.
45. Ortiz-Barahona A, Villar D, Pescador N, et al. Genome-wide identification of hypoxia-inducible factor binding sites and target genes by a probabilistic model integrating transcription-profiling data and in silico binding site prediction. Nucleic Acids Res 2010;38:2332–2345.
46. Semenza GL, Nejfelt MK, Chi SM, et al. Hypoxia-inducible nuclear factors bind to an enhancer element located 3′ to the human erythropoietin gene. Proc Natl Acad Sci USA 1991;88:5680–5684.
47. Yu J, Li JL, Zhang SY, et al. IGF-1 induces hypoxia-inducible factor 1 alpha-mediated GLUT3 expression through PI3K/Akt/mTOR dependent pathways in PC12 cells. Brain Res 2012;1430:18–24.
48. Tordjman R, Delaire S, Plouet J, et al. Erythroblasts are a source of angiogenic factors. Blood 2001;97:1968–1974.
49. Perelman N, Selvaraj SK, Batra S, et al. Placenta growth factor activates monocytes and correlates with sickle cell disease severity. Blood 2003;102: 1506–1514.
50. Brittain JE, Hulkower B, Jones SK, et al. Placenta growth factor in sickle cell disease: association with hemolysis and inflammation. Blood 2010;115:2014–2020.
51. Belcher JD, Marker PH, Weber JP, et al. Activated monocytes in sickle cell disease: potential role in the activation of vascular endothelium and vaso-occlusion. Blood 2000;96:2451–2459.